Supplemental Materials

Molecular Biology of the Cell

Duellberg et al.

SUPPLEMENTAL FIGURE LEGENDS

Supplemental Figure 1: (A) Steady state microtubule lifetime distributions. Cumulative distributions of the measured lifetimes as presented in Figure 1 for 0.5 mM and 10 mM $MgCl_2$, as indicated. The tubulin concentration was 10 μM. Inset: same distributions as histogram. (B) As (A) for measured average growth speeds.

Supplemental Figure 2: Catastrophe criterion. (A) For the quantification of delay times, kymographs were generated from raw movies. The sudden decrease in background intensity was used to determine the time point, when tubulin was removed (marked with a blue line). The position of the microtubule plus end at washout was then determined (here marked with a green arrowhead). The delay time was defined as the time it took for the microtubule to shrink 3 pixels (3x 120 nm = 360 nm). It was determined, using Image J, by drawing a line as indicated by the green line in the kymograph. (B) We compared the '360 nm offset' catastrophe criterion used here with our previously used '25% slope change' criterion (Duellberg *et al.*, 2016). For this test, we selected two datasets from our previous study (dataset 1 from Figure 1, 2 and dataset 2 from Figure 6 (Duellberg *et al.*, 2016)), which had been previously tracked automatically, and determined the delay time distributions using the two catastrophe criteria. This test produced essentially the same distributions, validating the catastrophe criterion used here.

Supplemental Figure 3: Fast microtubule depolymerisation speeds after catastrophe. Fast depolymerisation speeds were determined for the washout experiments shown in Figure 2, using kymograph analysis. The fast depolymerisation speeds are dictated by the $MgCl_2$ concentration of the washout buffer. Standard box plot representation (n> 38).

Supplemental Figure 4: Comparison of simulated delay times according to the defect model with the analytic approximation. Histogram of delay times until a catastrophe occurs after washout at 30 s, from a stochastic simulation of a multi-step defect model for 5000 microtubules, as described in the Methods. Simulated parameter values were k_{on} = 6 s^{-1}, k_{off} = k_{off2} = 0.5 s^{-1}, h = 0.15 s^{-1}. The red curve shows the corresponding theoretical distribution for the probability density function, as calculated in the Methods.

Supplemental Figure 5: Dependence of delay times on taper length and shape. (A, B) Linear taper: (A) Illustration of temporal decays of the maximum cap density after tubulin washout for the example caps shown in Figure 5B. The time courses calculated according to the 'taper – cap density' model show that the critical threshold (green dashed line) is reached faster for caps of microtubules with longer linear taper lengths and hence with lower maximum cap density at washout. **(B)** Illustration of the decrease of the delay times with linear taper length, for the example shown in (A). Parameter values used for the calculation according to the 'linear taper - cap density' model were k_m = 0.1 s^{-1}, v_g = 36 nm/s, v_s = 34nm/s , γ = 0.23. Five examples for L_t ranging from 0 nm to the comet length $L = v_g/k_m$. **(C, D) Gaussian taper: (C)** A taper model with a Gaussian length distribution was

examined for comparison, leading to an exponentially modified Gaussian cap density distribution. The plot shows how the distribution is affected by the Gaussian taper length, defined here as the distance between – 2 σ and + 2 σ of the taper structure. The same parameter values are used for calculating the Gaussian tapered cap model as for the linear taper model (shown in A, B, Figure 5B). The vertical blue line illustrates the comet length. **(D)** Dependence of the calculated delay times for the example in (C) on the taper length (numbers directly comparable to the linear taper model in (B)). The dashed blue line shows the comet length chosen for this example. Comparison of (B) and (D) shows that the exact shape of the taper does not strongly influence the predicted delay times.

Supplemental Table 1: Summary of input and output values from fits presented in Figure 4

[$MgCl_2$] (mM)	1.6		4		10	
Washout time (s)	35	160	35	160	35	160
Measured <Delay time> (s)	9.5 *(0.5)*	8.0 *(0.4)*	7.7 *(0.3)*	6.3 *(0.3)*	5.5 *(0.4)*	4.0 *(0.3)*
Growth speed, v_g (nm/s)	28 *(2)*		36 *(2)*		46 *(3)*	
Shrinkage speed, v_s (nm/s)	29 *(3)*		32 *(5)*		39 *(11)*	
Maturation rate, k_m (s^{-1})	0.1 *(0.01)*		0.1 *(0.01)*		0.1 *(0.01)*	
k_{on} (s-1) *partly constrained*	3.5		4.5		5.75	
k_{off1} (s-1) *partly constrained*	0.01		0.01		0.01	
k_{off2} = v_s/8nm *fixed*	3.62		4		4.875	
***h* (s^{-1})** *partly constrained*	0.1		0.1		0.1	
Predicted <Delay time> (s)	0.89	0.79	0.88	0.81	0.82	0.77
Alternative models. Unless specified, all other parameters are as above						
***h* (s^{-1})** *free*	0.0015		0.0015		0.0015	
Predicted <Delay time> (s)	8.1	6	7.0	5.7	7.0	5.2
2 defect criterion						
Predicted <Delay time> (s)	0.64	0.57	0.65	0.59	0.61	0.56
4 defect criterion						
Predicted <Delay time> (s)	1.1	1.0	1.1	1.0	1.0	0.97

Experimentally measured mean delay times (Figure 3) are summarised for the two washout times at the three magnesium concentrations tested, as indicated. Black values are experimental results (SE in bracket), blue parameters are derived from the fits (described below), red values are the predicted delay times. Growth speeds, v_g were determined from the trajectories before washout (see Methods). The slow shrinkage speed, v_s between tubulin washout and catastrophe could not be measured reliably by kymograph analysis used here. Instead the shrinkage speeds were calculated from shrinkage speeds measured previously using sub-pixel precision microtubule end tracking for two different magnesium concentrations (as presented in Fig.2 - Suppl Fig. 1C and Fig.6 - Suppl. Fig. 1C in) at the same tubulin concentration as used here (see Methods). Maturation rates k_m were determined in independent experiments spiked with Mal3-GFP (see Methods) using comet analysis. The defect model parameters

used for the fits in Figure 4 are: the rate constants, k_{on} and k_{off} before tubulin washout are free fit parameters but constrained by the growth speed, v_g. The dissociation constant after washout k_{off2} is determined by the shrinkage speed, v_s (division by the length of the tubulin subunit) and is fixed. The values for these rate constants are given per protofilament. The hydrolysis rate h is partly constrained by not being allowed to be smaller than the measured maturation rate, k_m. The maturation rate describes the disappearance of stabilizing EB sites at the microtubule end. Presently, it is not clear if these sites represent GTP or GDP-Pi tubulin or some intermediate state, but it is generally believed that this is not GDP tubulin (Maurer *et al.*, 2011; Zhang *et al.*, 2015). We therefore make the assumption that k_h is either the same as the maturation rate or that it is faster but that it cannot be slower. Predicted mean delay times are given in red. Other fits were made with an unconstrained hydrolysis rate, h, and with 2- and 4- critical defect versions of the model. The equation used for the PDF of the delay times according to the 3-defect model (see Methods) is

$$\frac{858\, e^{-(13Y+ht')}\left(e^{(Y+Zt_{wo})}-1\right)^2\left(R\, e^{ht'}-k_{on}+k_{off}\right)k_{off2}}{(66-143\, e^{Zt_{wo}}+78\, e^{2Zt_{wo}})\,R}$$

with

$$R = k_{on}-k_{off}+h, \qquad Y = k_{off2}\left(t'-\frac{(1-e^{-ht'})(k_{on}-k_{off})}{R\,h}\right), \qquad Z=\frac{k_{off}\,h}{R}$$

Supplemental Table 2: Summary of input and output values from fits presented in Figure 5

[$MgCl_2$] (mM)	1.6		4		10	
Washout time (s)	35	160	35	160	35	160
Measured <Delay time> (s)	9.5	8.0	7.7	6.3	5.5	4.0
Growth speed, v_g (nm/s)	28		36		46	
Shrinkage speed, v_s (nm/s)	29		32		39	
Maturation rate, k_m (s^{-1})	0.1		0.1		0.1	
Density threshold *free*	0.14 *(0.003)*		0.24 (*0.004*)		0.33 (*0.006*)	
Taper factor *free, shared*			0.047 (*0.003*)			
Predicted taper length [nm]	49 *(4.3)*	220 *(20)*	56 *(4.2)*	260 *(19)*	76 *(6.4)*	350 *(29)*
Predicted <Delay time> (s)	9.4 *(1.5)*	8.1 *(1.0)*	7.7 *(1.5)*	6.3 *(0.9)*	5.5 *(1.4)*	4.1 *(0.8)*

Experimentally measured mean delay times (Figure 3) are summarised for the two washout times at the three magnesium concentrations tested, as indicated. Growth speeds, v_g, the slow shrinkage speed, v_s between tubulin washout and catastrophe, and maturation rates k_m were determined as described in Supplemental table 1 and Methods and were fixed parameters in the 'taper - cap density' model (Methods) used for the global fit to the measured delay times. The maximum density thresholds (one per magnesium concentration) and the taper factor f_t (shared for all magnesium concentrations) are free fit parameters and the values for the best global fit are presented with their fit errors (in brackets). The predicted delay times and the calculated predicted taper lengths are given with their errors as calculated from error propagation. The predicted theoretical delay times for washout time 0 s (= no taper) are 9.82, 8.14 and 5.96 s for 1.6 mM, 4 mM and 10 mM $MgCl_2$, respectively (green line in Figure 5D and y-axis intercepts in Figure 5E.

A

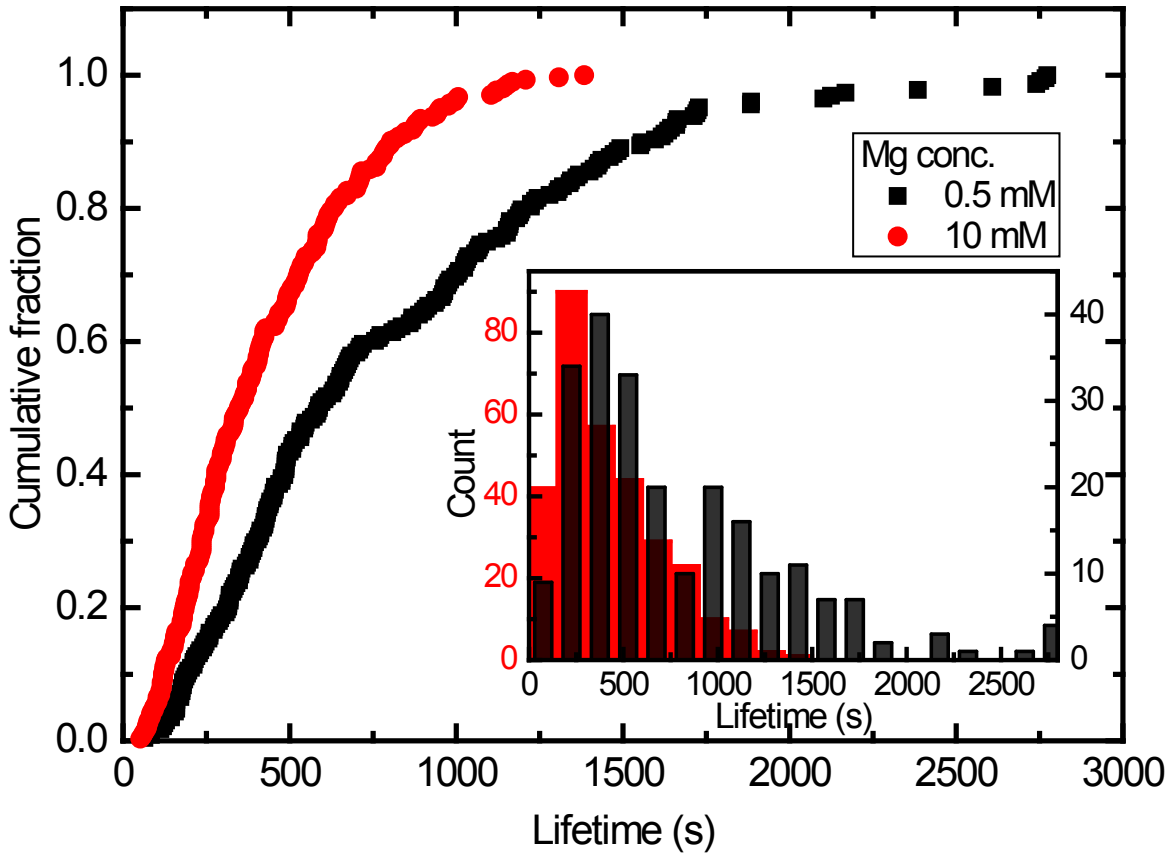
Cumulative fraction
Lifetime (s)
Mg conc.
0.5 mM
10 mM
Count
Lifetime (s)

B

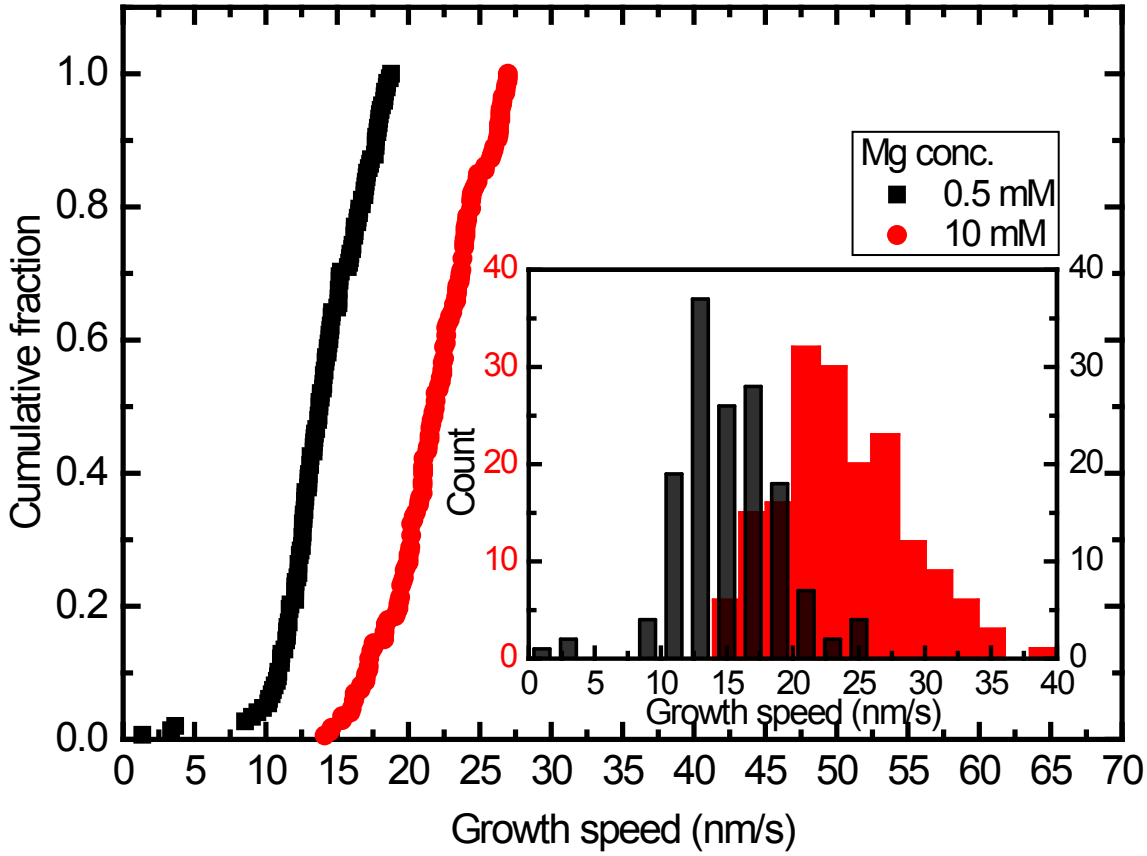
Cumulative fraction
Growth speed (nm/s)
Mg conc.
0.5 mM
10 mM
Count
Growth speed (nm/s)

A

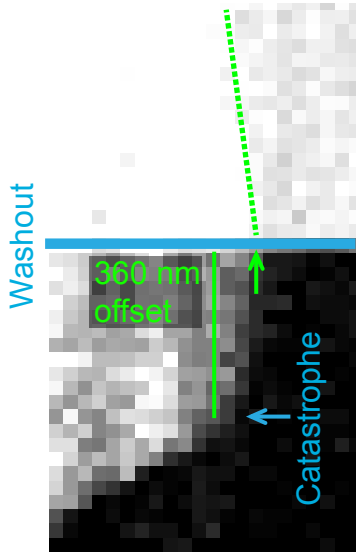
Washout
360 nm
offset
Catastrophe

B

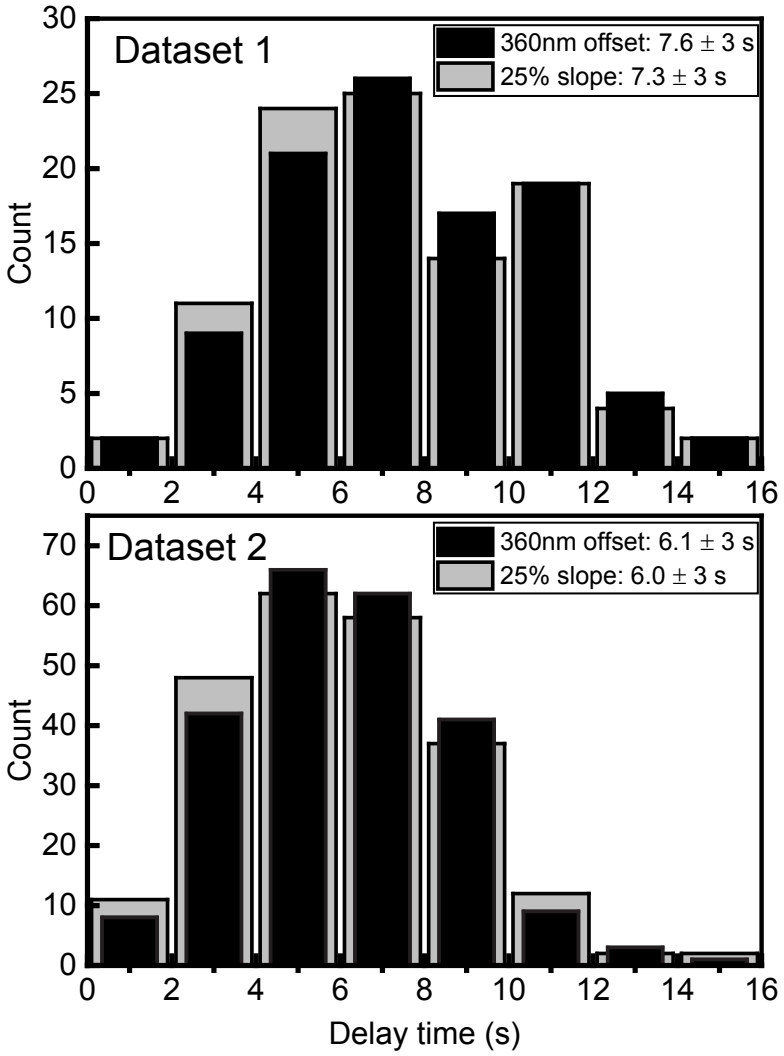
Dataset 1
360nm offset: 7.6 ± 3 s
25% slope: 7.3 ± 3 s
Count
Dataset 2
360nm offset: 6.1 ± 3 s
25% slope: 6.0 ± 3 s
Count
Delay time (s)

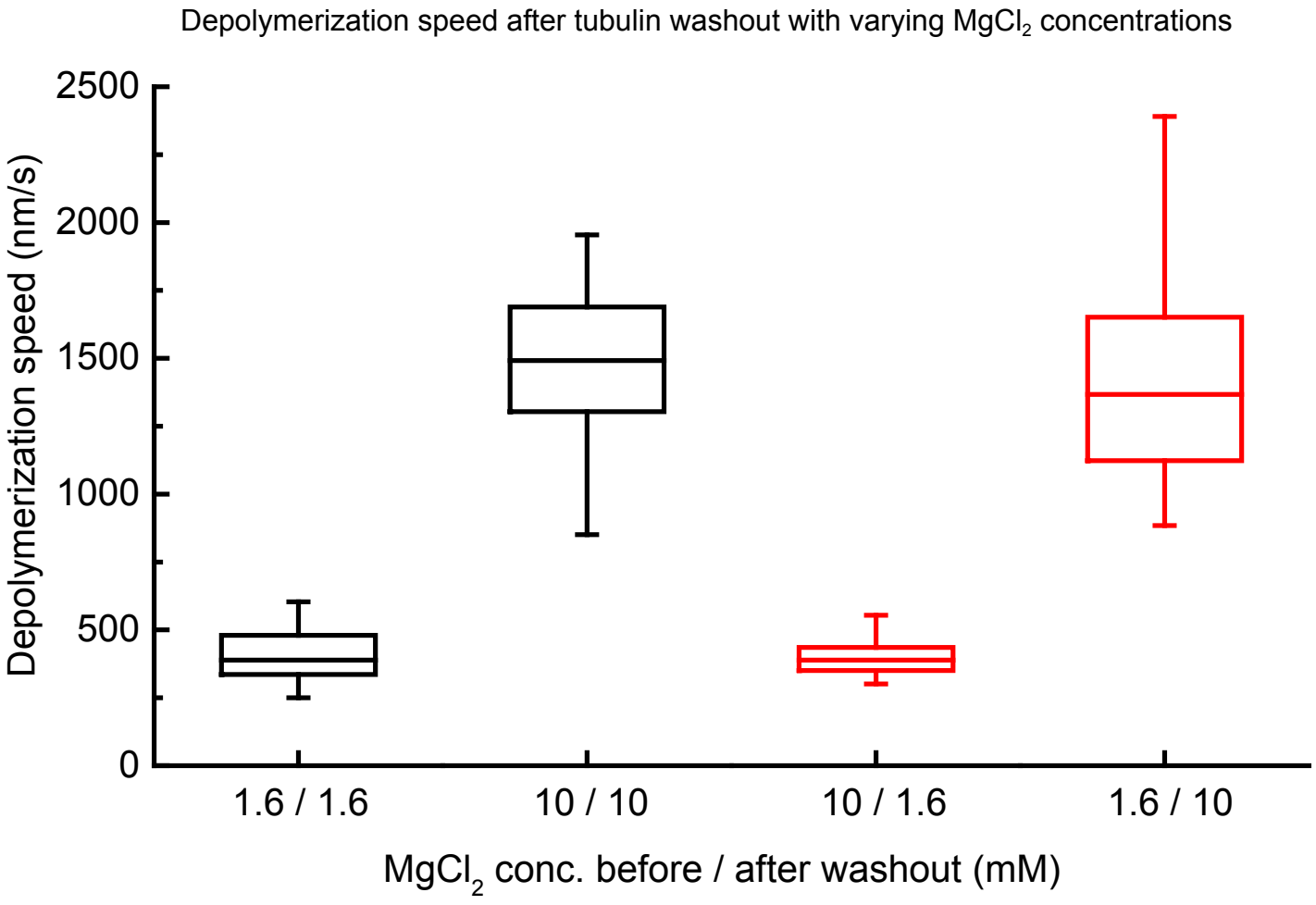
Depolymerization speed after tubulin washout with varying MgCl2 concentrations
Depolymerization speed (nm/s)
2500
2000
1500
1000
500
0
1.6 / 1.6
10 / 10
10 / 1.6
1.6 / 10
MgCl2 conc. before / after washout (mM)

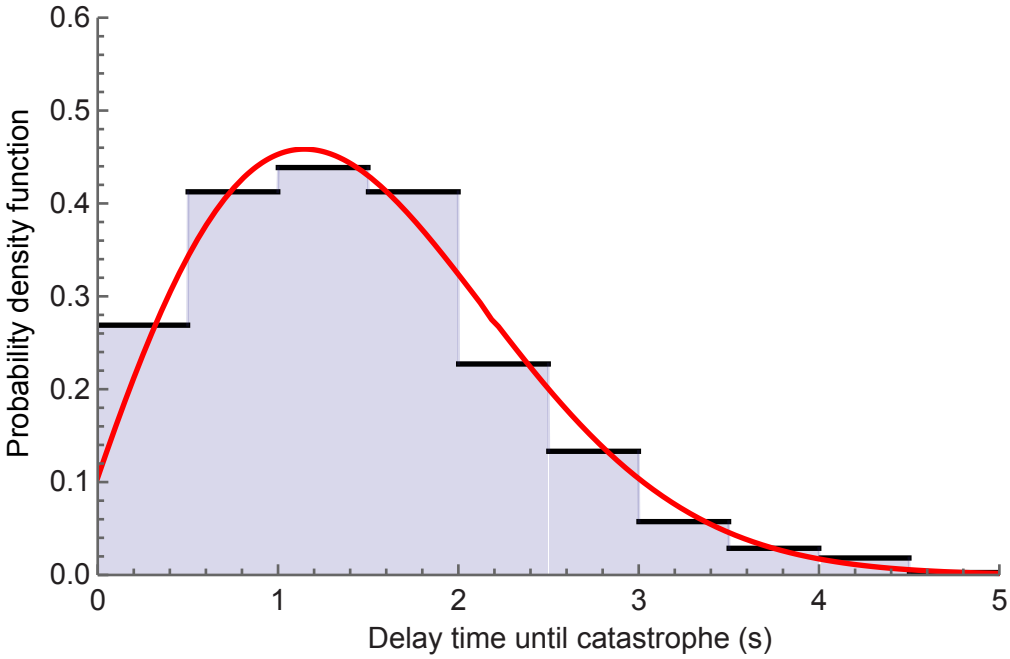
Probability density function
0.6
0.5
0.4
0.3
0.2
0.1
0.0
0
1
2
3
4
5
Delay time until catastrophe (s)

A Linear taper: Time evolution of maximum density after washout

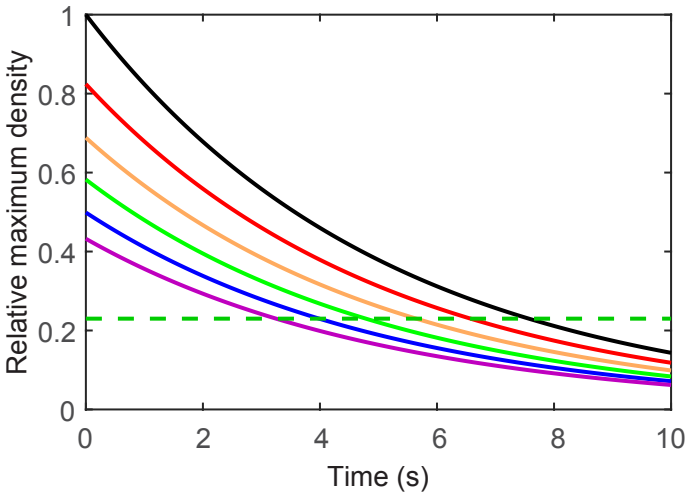

B Delay time vs linear taper length

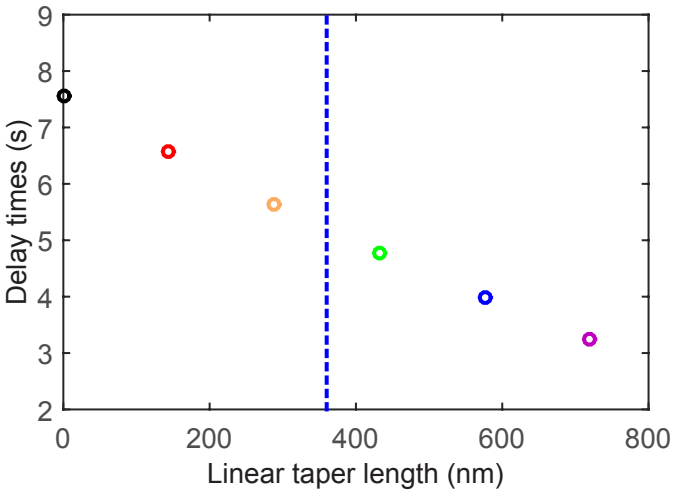

C Effect of gaussian taper on distribution of cap sites

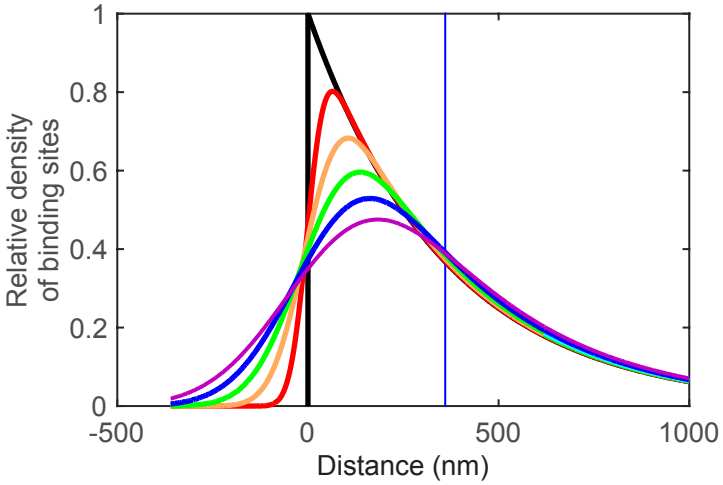

D Delay time vs gaussian taper length